An Inversion Method for the Exponential Radon Transform Based on the Harmonic Analysis of the Euclidean Motion Group

Can Evren Yarman and Birsen Yazıcı

Department of Electrical, Computer and System Engineering,
Rensselaer Polytechnic Institute,
110 8th St., Troy, NY 12180 USA

ABSTRACT

This paper presents a new method for exponential Radon transform inversion based on the harmonic analysis of the Euclidean motion group of the plane. The proposed inversion method is based on the observation that the exponential Radon transform can be modified to obtain a new transform, defined as the modified exponential Radon transform, that can be expressed as a convolution on the Euclidean motion group. The convolution representation of the modified exponential Radon transform is block diagonalized in the Euclidean motion group Fourier domain. Further analysis of the block diagonal representation provides a class of relationships between the spherical harmonic decompositions of the Fourier transforms of the function and its exponential Radon transform. The block diagonal representation provides a method to simultaneously compute all these relationships. The proposed algorithm is implemented using the fast implementation of the Euclidean motion group Fourier transform and its performances is demonstrated in numerical simulations.

Keywords: exponential Radon transform, Euclidean motion group, harmonic analysis, convolution representation

1. INTRODUCTION

The exponential Radon transform constitutes a mathematical model for imaging modalities such as x-ray tomography ($\mu = 0$), single photon emission tomography (SPECT) ($\mu \in \mathbb{R}$)[1, 2] , and optical polarization tomography of stress tensor field ($\mu \in \mathrm{i}\mathbb{R}$).[3]

For a uniform attenuation coefficient $\mu \in \mathbb{C}$, the exponential Radon transform of a compactly supported real valued function f over $\mathbb{R}^2$ is defined as

$$\mathcal{T}_\mu f(\boldsymbol{\theta}, t) = \int_{\mathbb{R}^2} f(\boldsymbol{x})\delta(\boldsymbol{x}\cdot\boldsymbol{\theta} - t)\mathrm{e}^{\mu \boldsymbol{x}\cdot\boldsymbol{\theta}^\perp} d\boldsymbol{x}, \tag{1}$$

where $t \in \mathbb{R}$, $\boldsymbol{\theta} = (\cos\theta, \sin\theta)^T$ is a unit vector on S^1 with $\theta \in [0, 2\pi)$ and $\boldsymbol{\theta}^\perp = (-\sin\theta, \cos\theta)^T$. We invert the exponential Radon transform by studying its invariance with respect to the Euclidean motions of the plane. Our analysis starts with the following modification of the exponential Radon transform:

$$\mathcal{T}'_\mu f(\boldsymbol{\vartheta}, r_1, r_2) = \mathcal{T}_\mu f(\boldsymbol{\vartheta}, -r_1)\mathrm{e}^{\mu r_2}, \qquad \boldsymbol{\vartheta} = (\cos\theta, -\sin\theta)^T,\ r_1, r_2 \in \mathbb{R}. \tag{2}$$

We refer to the resulting transform $\mathcal{T}'_\mu$ as the *modified exponential Radon transform*. We showed[7] that the modified exponential Radon transform can be expressed as a convolution over the Euclidean motion group of the plane.

In this paper, we present a new inversion algorithm for the exponential Radon transform based on this convolution representation. Analysis of the algorithm leads to circular harmonic decomposition type relationships[7] between the Fourier transforms of f and its exponential Radon transform which fall into the class of relationships presented by Metz and Pan[2] . Our derivation differs from the one presented in[2] that we used the underlying invariance of the exponential Radon transform with respect to the Euclidean motion group. The

Medical Imaging 2006: Physics of Medical Imaging, edited by Michael J. Flynn, Jiang Hsieh,
Proceedings of SPIE Vol. 6142, 61424A, (2006) · 1605-7422/06/$15 · doi: 10.1117/12.647807

presented algorithm can compute and incorporate all the circular harmonic decomposition type relationships simultaneously.

The rest of the paper is organized as follows: In Section 2, we introduce the Euclidean motion group of the plane and its Fourier transform. In Section 3, we present the convolution representation of the modified exponential Radon transform and its diagonalization. In Section 4, we described the reconstruction algorithm based on the diagonalization of the modified exponential Radon transform and the Fourier transform of the Euclidean motion group. In Section 5, we present numerical simulations and compared the performance of the proposed algorithm with the previously proposed algorithms[7] . Finally, in Section 6, we summarize our results and conclusion.

2. HARMONIC ANALYSIS OF THE EUCLIDEAN MOTION GROUP

2.1. Euclidean Motion Group

The rigid motions of $\mathbb{R}^2$ are made up of translations and rotations. Translations form the group $\mathbb{R}^2$ with group operation being the vector addition. Any rotation of $\mathbb{R}^2$ can be represented as an 2×2 unitary matrix parameterized by $\theta \in [0, 2\pi)$, R_θ, i.e.

$$R_\theta = \begin{bmatrix} \cos\theta & -\sin\theta \\ \sin\theta & \cos\theta \end{bmatrix}. \tag{3}$$

Rotations of $\mathbb{R}^2$ form the group $SO(2)$ with matrix product being the group operation.

The rigid motions of $\mathbb{R}^2$ form the group called the *Euclidean motion group* of the plane, denoted by $M(2)$. The elements of the group are 3×3 matrices of the form

$$(R_\theta, \boldsymbol{r}) = \begin{bmatrix} R_\theta & \boldsymbol{r} \\ \boldsymbol{0}^T & 1 \end{bmatrix}, \ \ R_\theta \in SO(2), \ \ \boldsymbol{r} \in \mathbb{R}^2, \tag{4}$$

parameterized by a rotation component θ and a translation component $\boldsymbol{r}$. The group operation of $M(2)$ is the usual matrix multiplications and inverse of an element is obtained by matrix inversion as $(R_\theta, \boldsymbol{r})^{-1} = (R_\theta^{-1}, -R_\theta^{-1}\boldsymbol{r})$. This defines $M(2)$ as the semidirect product of the additive group of $\mathbb{R}^2$ and special orthonormal group $SO(2)$, i.e. $M(2) = SO(2) \ltimes \mathbb{R}^2$.

2.2. Fourier Transform over the Euclidean Motion Group

Fourier transform over the Euclidean motion group, which we will also refer to as $M(2)$-Fourier transform for short, projects a square integrable function f over $M(2)$, $f \in L^2(M(2))$, onto the irreducible unitary representations $U^{(\lambda)}(g)$ of $M(2)$, where g is an element of $M(2)$ and λ is the frequency parameter. Each irreducible unitary representation corresponds to an invariant subspace of $L^2(M(2))$ parameterized by λ. Therefore $M(2)$-Fourier transform decomposes a given function as a direct sum of its projections over the invariant subspaces of $M(2)$.[9] This decomposition together with the homomorphism property of $U^{(\lambda)}(g)$,

$$U^{(\lambda)}(g_1 g_2) = U^{(\lambda)}(g_1) U^{(\lambda)}(g_2), \tag{5}$$

allows group convolution to be expressed as a multiplication in the Fourier domain. For a detailed treatment of the topic, we refer the reader to[9, 10] .

The irreducible unitary representations, $U^{(\lambda)}(g)$, of $M(2)$ over $L^2(M(2))$ is given by the following linear operators:

$$(U^{(\lambda)}(g)F)(\boldsymbol{s}) = \mathrm{e}^{-\mathrm{i}\lambda(\boldsymbol{r}\cdot\boldsymbol{s})} F(R_\theta^{-1}\boldsymbol{s}), \ \ F \in L^2(S^1), \tag{6}$$

where $g = (\theta, \boldsymbol{r}) \in M(2)$, $\boldsymbol{s}$ is a point on the unit circle S^1, $(\ \cdot\ )$ is the standard inner product over $\mathbb{R}^2$, and λ is a nonnegative real number.[10]

We can express the matrix elements $u_{mn}^{(\lambda)}(g)$ of $U^{(\lambda)}(g)$ using the *circular harmonics* $\{S_m\}$, which form an orthonormal basis of $L^2(S^1)$,[10, 11] as follows

$$u_{mn}^{(\lambda)}(g) = (S_m, U^{(\lambda)}(g)S_n) = \int_{S^1} \overline{S_m(\boldsymbol{\omega})} \mathrm{e}^{-\mathrm{i}\lambda \boldsymbol{r}\cdot\boldsymbol{\omega}} S_n(R_\theta^{-1}\boldsymbol{\omega}) d(\boldsymbol{\omega}). \tag{7}$$

Choosing the complex exponentials $\{\mathrm{e}^{\mathrm{i}n\psi}\}$, $n \in \mathbb{Z}$ as the orthonormal basis for $L^2(S^1)$, the matrix elements for the unitary representation $U^{(\lambda)}(g)$ of $M(2)$ become[10]:

$$u_{mn}^{(\lambda)}(g) = (\mathrm{e}^{\mathrm{i}m\psi}, U^{(\lambda)}(g)\mathrm{e}^{\mathrm{i}n\psi}) \tag{8}$$

$$= \frac{1}{2\pi}\int_0^{2\pi} \mathrm{e}^{-\mathrm{i}m\psi}\mathrm{e}^{-\mathrm{i}(r_1\lambda\cos\psi + r_2\lambda\sin\psi)}\mathrm{e}^{\mathrm{i}n(\psi-\theta)}d\psi, \qquad \forall m,n \in \mathbb{Z}. \tag{9}$$

Alternatively, $u_{mn}^{(\lambda)}(g)$ can be expressed as

$$u_{mn}^{(\lambda)}(g) = \mathrm{i}^{n-m}\mathrm{e}^{-\mathrm{i}[n\theta+(m-n)\phi]}J_{n-m}(\lambda r), \tag{10}$$

where $J_n(r)$ is the n^{th} order Bessel function.

The matrix elements of $U^{(\lambda)}(g)$ satisfy the following properties:

$$u_{mn}^{(\lambda)}(g^{-1}) = {u_{mn}^{(\lambda)}}^{-1}(g) = \overline{u_{nm}^{(\lambda)}(g)}, \tag{11}$$

$$u_{mn}^{(\lambda)}(g_1 g_2) = \sum_k u_{mk}^{(\lambda)}(g_1)u_{kn}^{(\lambda)}(g_2). \tag{12}$$

Furthermore, the matrix elements $u_{mn}^{(\lambda)}(g)$ of $U^{\lambda}(g)$ form a complete orthonormal system in $L^2(M(2))$.

Let $f \in L^2(M(2))$, then its $M(2)$-*Fourier transform* is defined as[9, 10]

$$\mathcal{F}_{M(2)}(f)(\lambda) = \widehat{f}(\lambda) = \int_{M(2)} f(g)U^{(\lambda)}(g^{-1})\ d(g), \tag{13}$$

where $g = (R_\theta, \boldsymbol{r})$, $d(g) = d\boldsymbol{r}d(\theta)$ is the normalized Haar measure on $M(2)$ with $d(\theta)$ is the normalized Haar measure on $SO(2)$,[12] and the *inverse* $M(2)$-*Fourier transform* is given by

$$\mathcal{F}_{M(2)}^{-1}(\widehat{f})(g) = f(g) = \frac{1}{(2\pi)^2}\int_0^\infty \mathrm{Trace}\left(\widehat{f}(\lambda)U^{(\lambda)}(g)\right)\lambda d\lambda. \tag{14}$$

The $M(2)$-Fourier coefficients are operator valued functions that can be expressed in terms of matrices given an orthonormal basis over $L^2(S^1)$. Given the matrix elements of the unitary representations, the $M(2)$-Fourier and inverse $M(2)$-Fourier transforms can be expressed as follows[9]:

$$\mathcal{F}_{M(2)}(f)_{mn}(\lambda) = \widehat{f}_{mn}(\lambda) = \int_{M(2)} f(g)u_{mn}^{(\lambda)}(g^{-1})d(g), \tag{15}$$

$$\mathcal{F}_{M(2)}^{-1}(\widehat{f}_{mn})(g) = f(g) = \frac{1}{(2\pi)^2}\int_0^\infty \sum_{m,n} \widehat{f}_{mn}(\lambda)u_{nm}^{(\lambda)}(g)\lambda^{N-1}d\lambda. \tag{16}$$

Using (15) and (9), the $M(2)$-Fourier matrix elements can be expressed as

$$\widehat{f}_{mn}(\lambda) = \frac{1}{(2\pi)^2}\int_0^{2\pi}\left(\left[\int_0^{2\pi}\left[\int_{\mathbb{R}^2} f(g)\mathrm{e}^{\mathrm{i}(r_1\lambda\cos\psi + r_2\lambda\sin\psi)}dr_1dr_2\right]\mathrm{e}^{\mathrm{i}m\theta}d\theta\right]\mathrm{e}^{-\mathrm{i}m\psi}\right)\mathrm{e}^{\mathrm{i}n\psi}d\psi. \tag{17}$$

Equation (17) shows that given $\{\mathrm{e}^{\mathrm{i}n\psi}\}_{n\in\mathbb{Z}}$ as the orthonormal basis for $L^2(S^1)$, computing the $M(2)$-Fourier transform of f is equivalent to computing four consecutive standard Fourier transforms. First two Fourier transforms are due to the integration over $\mathbb{R}^2$. The last two Fourier transforms are due to the integrations over $\theta \in [0, 2\pi)$ and $\phi \in [0, 2\pi)$.

For the rest of the paper, the orthonormal basis $\{S_m\}$ of $L^2(S^1)$ is assumed to be the complex exponential $\{\mathrm{e}^{im\phi}\}$.

Here, the properties of the $M(2)$-Fourier transform that are relevant to rest of our discussion are presented:

1. *Adjoint property:* Let $f \in L^2(M(2))$, then

$$\widehat{f^*}_{mn}(\lambda) = \overline{\widehat{f}_{nm}(\lambda)}, \tag{18}$$

where $f^*(g) = \overline{f(g^{-1})}$.

2. *Convolution property:* Let $f_1,\ f_2 \in L^2(M(2))$, and let $g = (R_\theta, \boldsymbol{r})$ and $h = (R_\phi, \boldsymbol{x})$. Convolution over $M(2)$ is defined by

$$(f_1 *_{M(2)} f_2)(g) = \int_{M(2)} f_1(h) f_2(h^{-1}g) d(h). \tag{19}$$

Then

$$\mathcal{F}_{M(2)}(f_1 * f_2)_{mn}(\lambda) = \sum_q \widehat{f}_{2mq}(\lambda)\ \widehat{f}_{1qn}(\lambda). \tag{20}$$

3. *$M(2)$-Fourier transform of $SO(2)$ invariant functions:* Let $f(g) = f(\boldsymbol{r}) \in L^2(\mathbb{R}^2)$, and define

$$\widetilde{f}_n(\lambda) = \int_0^{2\pi} \int_{\mathbb{R}^2} f(\boldsymbol{x}) \mathrm{e}^{-\mathrm{i}\lambda \boldsymbol{x}\cdot\boldsymbol{\theta}} \mathrm{e}^{in\theta}\, d\boldsymbol{x}\, d\theta, \tag{21}$$

to be the circular harmonic decomposition of the Fourier transform of f. Then

$$\widehat{f}_{mn}(\lambda) = \delta_{m0} \widetilde{f}_n(-\lambda), \qquad \lambda \geq 0, \quad m, n \in \mathbb{Z} \tag{22}$$

where δ_{0m} is the Kronecker delta function, equal to 1 if $m = 0$, and 0 otherwise. Hence, the $M(2)$-Fourier transform over $\mathbb{R}^2$ is equivalent to performing a standard Fourier transform followed by spherical harmonic decomposition. Similarly, the inverse $M(2)$-Fourier transform $\widehat{f}$ of $f \in L^2(\mathbb{R}^2)$, is obtained by reversing the order and the operations performed in the $M(2)$-Fourier transform.

4. *Band-limitedness* Let $\widehat{f}_{mn}(\lambda)$ be the $M(2)$-Fourier transform of a function $f \in L^2(M(2))$. Then f is said to be band-limited if there exist $m_0, n_0 \in \mathbb{Z}^+$, and $\lambda_0 > 0$ such that $\widehat{f}_{mn}(\lambda) = 0$ for $|m| > m_0$, $|n| > n_0$ and $\lambda > \lambda_0$.

   - If f is band-limited so is f^*.
   - If f_1 and f_2 are two band-limited functions, then $f_1 *_{M(2)} f_2$ is also band-limited.

3. MODIFIED EXPONENTIAL RADON TRANSFORM AS A CONVOLUTION

Recall that the exponential Radon transform of a compactly supported real valued function f over $\mathbb{R}^2$ is given by

$$\mathcal{T}_\mu f(\boldsymbol{\vartheta}, -r_1) = \int_{\mathbb{R}^2} f(\boldsymbol{x}) \delta(\boldsymbol{x} \cdot \boldsymbol{\vartheta} + r_1) \mathrm{e}^{\mu \boldsymbol{x}\cdot\boldsymbol{\vartheta}^\perp} d\boldsymbol{x}, \tag{23}$$

where $\mu \in \mathbb{C}$. Define Λ_μ to be

$$\Lambda_\mu(h) = \delta(\boldsymbol{x} \cdot \boldsymbol{e_1}) \mathrm{e}^{\mu\, \boldsymbol{x}\cdot\boldsymbol{e_2}}, \quad h = (R_\phi, \boldsymbol{x}) \in M(2). \tag{24}$$

Then the convolution of Λ_μ with f^* gives the modified exponential Radon transform of f:

$$\begin{aligned}(\Lambda_\mu *_{M(2)} f^*)(g) &= \int_{\mathbb{R}^2} f(\boldsymbol{x})\delta((R_\theta \boldsymbol{x}+\boldsymbol{r})\cdot \boldsymbol{e_1})\mathrm{e}^{\mu\,(R_\theta \boldsymbol{x}+\boldsymbol{r})\cdot \boldsymbol{e_2}} d\boldsymbol{x}, \qquad g=(R_\theta,\boldsymbol{r})\in M(2)\\ &= \int_{\mathbb{R}^2} f(\boldsymbol{x})\delta(R_\theta \boldsymbol{x}\cdot \boldsymbol{e_1}+r_1)\mathrm{e}^{\mu\, R_\theta \boldsymbol{x}\cdot \boldsymbol{e_2}+\mu r_2} d\boldsymbol{x}\\ &= \int_{\mathbb{R}^2} f(\boldsymbol{x})\delta(\boldsymbol{x}\cdot\boldsymbol{\vartheta}+r_1)\mathrm{e}^{\mu\,\boldsymbol{x}\cdot\boldsymbol{\vartheta}^\perp+\mu r_2} d\boldsymbol{x}\\ &= \mathrm{e}^{\mu r_2}\mathcal{T}_\mu f(\boldsymbol{\vartheta},-r_1) = \mathcal{T}'_\mu f(g). \end{aligned} \tag{25}$$

This is equivalent to say that the modified exponential Radon transform of a function is obtained by taking integral along a traversed weighted line, where the integration measure along the line is given by Λ_μ. The exponential Radon transform $\mathcal{T}_\mu f$ can be viewed as a restriction of the convolution $\Lambda_\mu *_{M(2)} f^*$

$$\begin{aligned}(\Lambda_\mu *_{M(2)} f^*)(g)\big|_{r_2=0} &= \mathcal{T}_\mu f(\boldsymbol{\vartheta},-r_1)\mathrm{e}^{\mu\, r_2}\big|_{r_2=0}\\ &= \mathcal{T}_\mu f(\boldsymbol{\vartheta},-r_1), \quad g=(R_\theta,\boldsymbol{r}),\end{aligned} \tag{26}$$

where $\boldsymbol{r}=(r_1,r_2)^T$ and $\boldsymbol{\vartheta}={R_\theta}^T\boldsymbol{e_1}$. Therefore inversion of the modified exponential Radon transform is equivalent to the inversion of modified exponential Radon transform.

Using the convolution property of the $M(2)$-Fourier transform and $SO(2)$ invariance of f, in $M(2)$-Fourier domain (25) becomes

$$\widehat{\mathcal{T}'_\mu f}_{mn}(\lambda) = \sum_q \overline{\widehat{f}_{qm}(\lambda)}\widehat{\Lambda_\mu}_{qn}(\lambda) \tag{27}$$

$$= \overline{\widehat{f}_{0m}(\lambda)}\widehat{\Lambda_\mu}_{0n}(\lambda), \quad m,n\in\mathbb{Z}. \tag{28}$$

Equations (27) and (28) provides block diagonal and diagonal representation of the modified exponential Radon transform in the $M(2)$-Fourier domain, respectively, where each block is indexed by $\lambda \geq 0$.

Circular Harmonic Decomposition Type Relationships

Substituting the values of $\widehat{\mathcal{T}_\mu f}_{mn}(\lambda)$ and $\widehat{\Lambda_\mu}_{0n}(\lambda)$

$$\widehat{\mathcal{T}_\mu f}_{mn}(\lambda) = \lambda^{-1}\left[\widetilde{\mathcal{T}_\mu f}_{-m}(\sqrt{\lambda^2+\mu^2})\gamma_\mu^{n-m} + (-1)^{n-m}\widetilde{\mathcal{T}_\mu f}_{-m}(-\sqrt{\lambda^2+\mu^2})\gamma_\mu^{-(n-m)}\right] \tag{29}$$

$$\widehat{\Lambda_\mu}_{0n}(\lambda) = \delta_{0m}\lambda^{-1}\left((-1)^n\gamma_\mu^{-n}+\gamma_\mu^n\right), \tag{30}$$

in (28), where $\gamma_\mu = \frac{\lambda}{\sqrt{\lambda^2+\mu^2}+\mu}$ and

$$\widetilde{\mathcal{T}_\mu f}_n(\lambda) = \int_0^{2\pi}\int_{\mathbb{R}} \mathcal{T}_\mu f(\boldsymbol{\theta},t)\mathrm{e}^{-\mathrm{i}\lambda t}\mathrm{e}^{\mathrm{i}n\theta}\,dt\,d\theta, \tag{31}$$

and using the $SO(2)$ invariance of f, we obtain

$$\widetilde{f}_m(\lambda) = \rho_n\gamma_\mu^m\widetilde{\mathcal{T}_\mu f}_m(\sqrt{\lambda^2+\mu^2}) + (1-\rho_n)(-\gamma_\mu)^{-m}\widetilde{\mathcal{T}_\mu f}_m(-\sqrt{\lambda^2+\mu^2}), \tag{32}$$

where $\rho_n = \frac{\gamma_\mu^n}{(-1)^n\gamma_\mu^{-n}+\gamma_\mu^n}$.

Taking complex conjugate of both sides of (32) and negating the signs of k and λ, one obtains the identity

$$\gamma_\mu^m\widetilde{\mathcal{T}_\mu f}_m(\sqrt{\mu^2+\lambda^2}) = (-1)^m\gamma_\mu^{-m}\widetilde{\mathcal{T}_\mu f}_m(-\sqrt{\mu^2+\lambda^2}), \tag{33}$$

which substituting back in (32) leads to the relationship

$$\widetilde{f}_m(\lambda) = \gamma_\mu^m \widetilde{\mathcal{T}_\mu f}_m(\sqrt{\mu^2+\lambda^2}). \tag{34}$$

(34) was first presented by Tretiak et al. ((33) in[1]), Hawkins et al. ((25) in[5]) and Inouye et al. ((13) in[6]) by performing circular harmonic decomposition of the radial Fourier transform of $\mathcal{T}f$:

$$\widetilde{\mathcal{T}_\mu f}_m(\lambda) = \left(\frac{\lambda+\mu}{\lambda-\mu}\right)^{m/2} \widetilde{f}_m(\sqrt{\lambda^2-\mu^2}), \tag{35}$$

By replacing λ with $\sqrt{\lambda^2+\mu^2}$, (35) is equivalent to (34):

$$\widetilde{f}_m(\lambda) = \left(\frac{\sqrt{\lambda^2+\mu^2}-\mu}{\sqrt{\lambda^2+\mu^2}+\mu}\right)^{m/2} \widetilde{\mathcal{T}_\mu f}_m(\sqrt{\lambda^2+\mu^2}) = \gamma_\mu^m \widetilde{\mathcal{T}_\mu f}_m(\sqrt{\lambda^2+\mu^2}). \tag{36}$$

Using (34) and (33), Metz et al. took a weighted sum approach to obtain

$$\widetilde{f}_m(\lambda) = \omega\gamma_\mu^m \widetilde{\mathcal{T}_\mu f}_m(\sqrt{\lambda^2+\mu^2}) + (1-\omega)(-1)^m \gamma_\mu^{-m} \widetilde{\mathcal{T}_\mu f}_m(-\sqrt{\lambda^2+\mu^2}), \tag{37}$$

which for different choices of the weighting factor ω leads to different Fourier type relationships between f and $\mathcal{T}_\mu f$ presented in[1,4–6].

Notice that our notation differs from those in[1,2,5,6], due to the definitions of the exponential Radon transform based on the convention μ or $-\mu$, and/or the spherical harmonic decomposition where $\widetilde{f}_m$ and $\widetilde{\mathcal{T}_\mu f}_m$ in those works respectively correspond to $\widetilde{f}_{-m}$ and $\widetilde{\mathcal{T}_\mu f}_{-m}$ in our work.

4. INVERSION OF EXPONENTIAL RADON TRANSFORM AND THE RECONSTRUCTION ALGORITHM

Previously[7], we presented two reconstruction algorithms based on (27) and (28), which simultaneously combined the relationships (32) for various n values. Here, we will provide an alternative reconstruction algorithm which is based on averaging (28) over n, and hence simultaneously combines the relationships (32) for various n values.

Averaging (28) over n $\widehat{f}$ can be recovered by

$$\widehat{f}_{0m}(\lambda) = \overline{\left(\frac{\sum_{n=N_0}^{N} \widehat{\mathcal{T}'_\mu f}_{mn}(\lambda)}{\sum_{n=N_0}^{N} \widehat{\Lambda_\mu}_{0n}(\lambda)}\right)}, \qquad N_0 \leq N, \quad N_0, N \in \mathbb{Z}. \tag{38}$$

We implemented our reconstruction algorithm based on the inversion formula (38) in four steps, which is summarized in the following diagram:

$$\begin{array}{ccccc} f & \xrightarrow{\mathcal{T}} & \mathcal{T}_\mu f & \xrightarrow[1]{\times e^{\mu r_2}} & \mathcal{T}'_\mu f \\ & \nwarrow^{4}_{\mathcal{F}^{-1}_{M(2)}} & & & \downarrow 2 \; \mathcal{F}_{M(2)} \\ & & \widehat{f}_{0m} & \xleftarrow[3]{(38)} & \widehat{\mathcal{T}'_\mu f}_{mn} \end{array} \quad . \tag{39}$$

1. As the first step, we extend the exponential Radon transform of f to modified exponential Radon transform over $M(2)$ by (2), multiplication of $\mathcal{T}_\mu f$ by $e^{\mu r_2}$.
2. In the second step, we take $M(2)$-Fourier transform of the modified exponential Radon transform.
3. In third step, we compute the $M(2)$-Fourier coefficients of f by (38).

4. Finally, in the fourth step, we take the inverse $M(2)$-Fourier transform to obtain f.

In the second and fourth steps of the proposed reconstruction algorithm we used a fast $M(2)$-Fourier transform algorithm based on equation (17). For a detailed description of the fast $M(2)$-Fourier transform algorithm we refer the reader to[8, 13, 15] .

Note that as long as $\sum_{n=N_0}^{N} \widehat{\Lambda_{\mu 0n}}(\lambda) \gg 0$ the proposed algorithm does not require any regularization. However, this requires computation of sufficient number of $M(2)$-Fourier coefficients, which can be simultaneously computed using $M(2)$-Fourier transform.

5. NUMERICAL SIMULATIONS

We performed numerical simulations on a two-dimensional Shepp-Logan phantom image corresponding to a region of $13.1 \times 13.1\text{cm}^2$, discretized by 129×129 pixels. We choose $\mu = 0.154\text{cm}^{-1}$, however the proposed reconstruction algorithm can be used for any complex μ. We previously studied the case for $\mu = 0$ in[14] and $\mu = \text{i}0.154\text{cm}^{-1}$ in[7] .

Figure 1 shows reconstructed images using the proposed algorithm for $\mu = 0.154\text{cm}^{-1}$ using multiple n values, where $n = -64, \ldots, 64$. The reconstructed images suggests that the proposed method induces less artifact when compared to the reconstructed images using the reconstruction algorithms proposed in[7] .

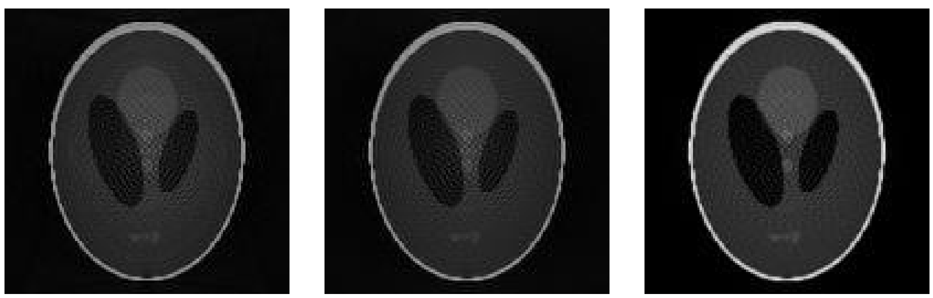

(a) (b) (c)

Figure 1. Reconstruction of the modified Shepp-Logan phantom of size $13.1 \times 13.1cm^2$ for $\mu = 0.154\text{cm}^{-1}$ and $n = -64, \ldots, 64$ using (a) *Algorithm 1* of [7] , (b) *Algorithm 2* of [7] , and (c) proposed algorithm.

6. CONCLUSION

In this work, we present a new reconstruction algorithm for the inversion of the exponential Radon transform based on harmonic analysis of the Euclidean motion group. The proposed algorithm starts with the modification of the exponential Radon transform. Then the inversion formula is obtained by diagonalizing the convolution representation of the modified exponential Radon transform in the $M(2)$-Fourier domain. Once the $M(2)$-Fourier coefficients of the function are computed using the inversion formula, the function is obtained by $M(2)$-Fourier inversion. We showed the performance of the proposed algorithm with numerical simulations. For $\mu = 0.154\text{cm}^{-1}$, visual comparison shows that the proposed algorithm is comparable or better than the previously[7] proposed algorithms.

REFERENCES

1. O. Tretiak and C. Metz, "The exponential radon transform," *SIAM J. Appl. Math.* **39**, pp. 341–354, 1980.
2. C. Metz and X. Pan, "A unified analysis of exact methods of inverting the 2-d exponential Radon transform, with implications for noise control in spect," *IEEE Transactions on Medical Imaging* **14**, pp. 643–658, 1995.
3. A. Puro, "Cormack-type inversion of exponential Radon transform," *Inverse Problems* **17**, pp. 179–188, 2001.

4. S. Bellini, M. Piancentini, C. Cafforio, and F. Rocca, "Compensation of tissue absorption in emission tomography," *IEEE Transactions on Acoustics, Speech and Signal Processing* **ASSP-27**, pp. 213–218, 1979.
5. G. W. Hawkins, P. K. Leichner, and N.-C. Yang, "The circular harmonic transform for SPECT reconstruction and boundary conditions on the fourier transform on the sinogram," *IEEE Transactions on Medical Imaging* **7**, pp. 135–148, 1988.
6. T. Inouye, K. Kose, and A. Hasegawa, "Image reconstruction algorithm for single-photon-emission computed tomography with uniform attenuation," *Phys. Med. Biol.* **34**, pp. 299–304, 1989.
7. C. Yarman and B. Yazıcı, "Exponential Radon transform inversion based on harmonic analysis of the Euclidean motion group," in *Proceedings of IEEE International Conference on Image Processing 2005*, 2005.
8. A. Kyatkin and G. Chirikjian, "Algorithms for fast convolutions on motion groups," *Applied Computational Harmonic Analysis* **9**, pp. 220–241, 2000.
9. M. Sugiura, *Unitary Representations and Harmonic Analysis*, Kodansha, Tokyo, 1975.
10. N. J. Vilenkin, *Special functions and the theory of representations*, American Mathematical Society, Providence, RI, 1988.
11. R. T. Seeley, "Spherical harmonics," *The American Mathematical Monthly* **73**, pp. 115–121, 1966.
12. F. Natterer, *The Mathematics of Computerized Tomography*, Wiley-Teubner, New York, NY, 1986.
13. C. Yarman and B. Yazıcı, "Radon transform inversion via Wiener filtering over the Euclidean motion group," in *Proceedings of IEEE international Conference on Image Processing 2003*, **2**, pp. 811–814, (Barcelona, Spain), 2003.
14. C. Yarman and B. Yazıcı, "Radon transform inversion based on harmonic analysis of the Euclidean motion group," in *Proceedings of IEEE International Conference on on Acoustics, Speech, and Signal Processing 2005*, 2005.
15. C. Yarman and B. Yazıcı, "A Wiener filtering approach over the Euclidean motion group for Radon transform inversion," in *Proceedings of SPIE Medical Imaging 2003*, **5032**, pp. 1884–1893, (San Diego, CA), May 2003.